Hybrid Binary-Real GA Optimization Approach for Breast Microwave Tomography

A. Sabouni [1], A. Ahtari [2], S. Noghanian [3], G. Thomas [4], and S. Pistorius [5]

[1] Department of Electrical Engineering and Physics,
Wilkes University, Wilkes-Barre, PA, 18766, USA
abas.sabouni@wilkes.edu

[2] Invenia Technical Computing Company, Manitoba, Winnipeg, MB, R3T 6A8, Canada
ali.ashtari@invenia.ca

[3] Department of Electrical Engineering,
University of North Dakota, Grand Forks, ND, 58203, USA
sima.noghanian@engr.und.edu

[4] Department of Electrical and Computer Engineering, University of Manitoba
Winnipeg, MB, R3T 5V6, Canada
gabriel.thomas@ad.umanitoba.ca

[5] Department of Physics and Astronomy, University of Manitoba, Winnipeg, MB, R3T 5V6, Canada
stephen.pistorius@cancercare.mb.ca

Abstract **─** A microwave tomography imaging system, which uses a hybrid binary-real genetic algorithm (GA) is described in this work. This method utilizes global optimization for solving the inverse scattering problem based on hybrid version of GA, which is the combination of both real and binary-coded GA. This method is principally aimed at breast imaging for the detection of malignant tumors. The proposed technique is based on a time-domain inverse solver, which uses the multi-illumination technique and includes the dispersive and heterogeneous characteristic of the breast tissues. In this algorithm, real-coded GA acts as a regularizer for binary-coded GA and rejects the non-true solutions. The proposed technique is validated using a numerical breast phantom created based on magnetic resonance imaging (MRI) of actual patients. The results are compared with non-hybrid binary and real GAs and the superior efficiency of the proposed method over the methods that solely employ real or binary GA is illustrated.

Index Terms - Breast cancer imaging, heterogeneous and dispersive breast tissue, hybrid binary-real GA optimization, inverse scattering problem, and microwave tomography.

I. INTRODUCTION

Traditional inverse scattering methods usually remove the ill-posed solutions by assuming a smooth profile [1]. This often causes the removal of the correct solution because in many applications, such as breast imaging, the dielectric profile being imaged is not smooth. In this paper, a new approach for treating the ill-posedness is proposed that uses *a-priori* information for regularization. It involves incorporating realistic assumptions about the breast, based on the measurements of breast dielectric properties. The authors developed the numerical simulation method based on the frequency dependence finite-difference time-domain ($(FD)^2TD$) and binary-coded genetic algorithm for detecting breast cancer [2]. The contribution of this paper is to

Submitted On: Feb. 26, 2013
Accepted On: Aug. 29, 2013

1054-4887 © 2013 ACES

demonstrate the ability of microwave tomography (MWT) technique, based on numerical methods for solving partial differential equations (PDEs) such as $(FD)^2TD$ and global optimization methods such as real and binary coded genetic algorithm (GA). To the best of our knowledge, this is the first attempt in using the combination of $(FD)^2TD$ and hybrid GA to reconstruct the location, shape, and dielectric properties of heterogeneous and dispersive media.

The previous technique presented in [2] uses $(FD)^2TD$ and binary GA for reconstructing the image and it works for simple structures of tissue composition. The RGA in the hybrid GA technique presented in [3] was based on optimizing two variables (permittivity and conductivity values) for each cell within the search space, while in the current paper the RGA is based on optimizing only one parameter (water content). In this paper the proposed technique is extended to objects with large distribution of dielectric properties, which includes the water dependency of dielectric properties of breast tissues using $(FD)^2TD$/hybrid-GA. Furthermore, the examples in previous paper were only hypothetical cases, while in this paper the proposed technique is evaluated using model driven from magnetic resonance imaging (MRI) data. In [4] the authors evaluated the real and binary GA with respect to the speed of convergence for limited number of generations for microwave imaging. The study of noise effects on $(FD)^2TD$/GA algorithm for solving the inverse scattering problem for heterogeneous and dispersive object is presented in [5].

The paper is organized as follows: in section II, we provide the notation and methodology. In section III, we cast the MWT problem as an optimization problem, where in an appropriate cost-function is to be minimized. Within this framework, we explain the use of hybrid GA as an optimization method in details. Section IV shows inversion results from synthetic data, followed by conclusion in section V.

II. METHODOLOGY

The problem's geometry is depicted in Fig. 1 where Ω is the imaging domain (or search space domain), which is occupied by single or multiple scatterers and V is the problem domain where the scattered field is collected. The Object of Interest (OI) is surrounded by measurement probes that areable to acquire samples of the scattered field outside the imaging domain at the observation points.

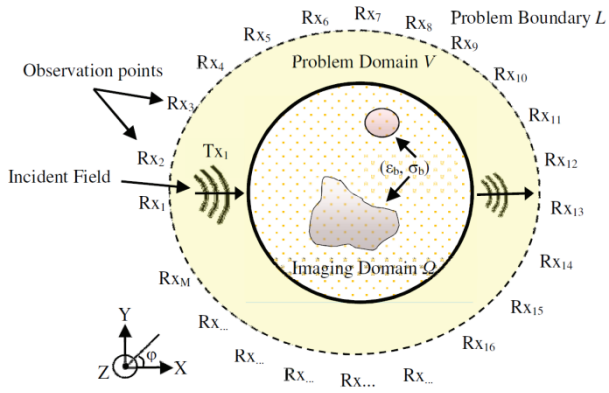

Fig. 1.Geometry of the MWT.

The region Ω is illuminated by a set of transverse magnetic (TM) fields (incident fields), denoted by E_i^{inc}, $i=1,2,3,...,N$ (N is the maximum number of illumination angles). The scattered field is measured around the object. The value of the scattered field is denoted by $E_{ij}^{scat}(r)$, $j=1,2,...,M$, and $i=1,2,3,...,N$ where the index j denotes the jth measurement point (observation point), located at different angles around the object. Since there are M measurement points and N incident angles, the scattered field can be stored in a matrix of size $N\times M$. In this paper, we consider the OI to be infinitely long in the z-direction (this creates a 2D problem). This approximation is made for efficiency in terms of runtime and memory. In fact, the behavior of the electric field within a 2D environment can be repeatedly evaluated very quickly, while this evaluation is much slower for 3D problems. This allows the iterative imaging algorithm to converge to a solution in a reasonable amount of time. In the framework of 2D inversion algorithms, we consider the TM polarization for illumination. In particular, we consider TM to z (TMz). This polarization is often used for 2D MWT [6, 7]. It should be noted that there is recent evidence that TE (transverse electric) polarization might provide better imaging results [8], however to the best of the author's knowledge, there is currently no TE MWT system capable of collecting all three components of the field.

III. MWT METHOD USING $(FD)^2TD$ AND GA

MWT is based on solving an inverse scattering problem. The most common way to solve the inverse scattering problems is to formulate it as a minimization problem. The cost-function is evaluated using the difference between the measured and predicted scattered fields for a particular choice of the material parameters (equation (1)). We propose to calculate the simulated scattered field at the observation points using ($(FD)^2TD$). This method has been selected due to the fact that the dispersive characteristic of material can be easily taken into account [9-12]. The GA is chosen for global optimization methods for optimizing the cost-function. The reason stems from the fact that the GA is able to deal with discrete cost-functions with multiple minima and it is possible to parallelize it so it reduces the computational time barrier in using global optimization. Equation (1) shows the proposed cost-function,

$$fitness = -\frac{1}{N}\sum_{i=1}^{N}\left|\sum_{f=f_1}^{f_2}\sum_{m=1}^{M}\frac{(E_{m,f,i}^{meas.}-E_{m,f,i}^{simu.})^2}{(E_{m,f,i}^{meas.})^2}\right| \quad (1)$$

where $E_{m,f,i}^{meas.}$ is the measured scattered electric fields, $E_{m,f,i}^{simu.}$ is the simulated scattered fields corresponding to the estimated dielectric properties of the imaging domain obtained by performing a forward simulation, M is the total number of observation points, and N is the total number of transmitters. In equation (1), f refers to different frequencies within f_1 to f_2 sampling frequency band. Increasing the number of observation points increases the possibility of convergence; however, there is a practical limit on the number of observation points. This is due to the limited space and mutual coupling between antennas. To mitigate the ill-posedness of the problem, a multi-illumination system is adopted to collect sufficient amount of data. This approach is based on the use of illuminating electromagnetic source at multiple angles around the observation domain where the scattered electromagnetic field is measured. Mainly, by illuminating the OI with a source at multiple angles, different values of the scattered field are measured.

A. Hybrid genetic algorithm

In inverse problem we propose to find the solution by minimizing the cost-function by using hybrid GA. Hybrid GA combines two different GAs: binary-coded GA (BGA) and real-coded GA (RGA). The BGA and RGA will be discussed separately in the following sections and then we will introduce the hybrid GA, which is the combination of BGA and RGA.

1) Binary-coded GA (BGA):

In BGA optimization, the region is discretized into a number of cells (n). One gene is the type of the specific material and it is distinguished by the Debye parameters. We designed a BGA that considers only limited material types taken from a look-up table, instead of randomly selecting the dielectric properties. The look-up table is created based on *a-priori* information and can be modified for different applications. Since the optimization variables are discrete with integer values, a coding procedure is needed. Each tissue type is represented by a string of q bits, where $q=log_2(L)$ and L is the total number of different tissue types. For example, if we assume four tissue types (fatty, transitional, fibro-glandular, and malignant tumour) then $L=4$ and $q=2$. After the discretization of the investigation domain (Fig. 2), the number of cells (n) multiplied by the number of bits (q) (that is assigned to each material) will be the size of one chromosome ($q\times n$). Therefore, if the OI is divided into n cells and in the look-up table for each material, two bits are assigned, then the size of the chromosome will be $2n$ bits. The number of unknowns for optimization depends on the number of cells in the investigation domain. Generally, in BGA, as the number of parameters increases, the convergence rate decreases and the memory requirement increases.

2) Real-coded GA (RGA)

In RGA optimization, the chromosome is a floating point number. In the proposed RGA the enclosed imaging domain is discretized into the same number of cells as BGA. Each cell corresponds to a tissue type. Tissue types are differentiated based on their dielectric properties using Debye model [13, 14] (see Table I).

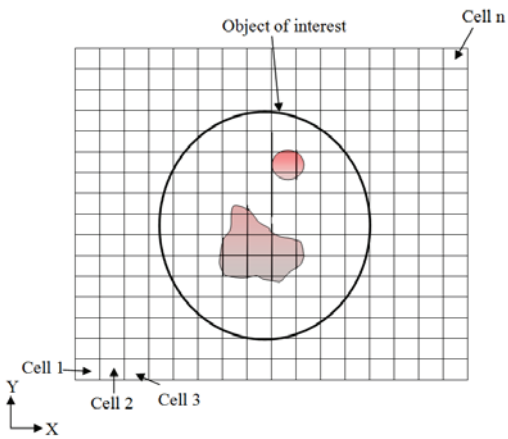

Fig. 2. Discretized the imaging domain for MWT.

Therefore each cell has a set of Debye parameter ($D_j j=1,2,..n$). j is the index to the cell location (Fig. 2). In conventional RGA, each element is initialized with parameters within the desired range. Depending on the application, the boundary of the permittivity and conductivity is determined. Each gene is a random number picked from a uniform distribution: ($\varepsilon_1<\varepsilon_j<\varepsilon_2$) and ($\sigma_1<\sigma_j<\sigma_2$), where ε_1 and ε_2 are the minimum and maximum possible values of the relative permittivity and σ_1 and σ_2 are minimum and maximum values for conductivity. It should be noted that this maximum and minimum number can be defined at a single-frequency, which will not work for a dispersive object. Each gene represents a variable of the problem without any coding or decoding procedure. An array of genes that shows the dielectric properties distribution for an entire imaging domain makes a chromosome. Therefore, for n cells each chromosome has n floating point numbers. Increasing n means that the resolution of imaging domain, and therefore, the search space is increased.

3) Hybrid GA (HGA):

The RGA-based procedure is very slow to converge, and the BGA-based procedure is not able to "fine-tune" the optimum solution. Each of them has some advantages and disadvantages. In fact, the RGA alone might be able to converge to the solution, but it is a laborious and time consuming process. On the contrary, the proposed BGA requires a limited number of possible dielectric properties that may not be realistic in some applications. To overcome these problems, a hybrid method (HGA) combining the BGA and RGA is introduced.

Figure 3 shows the block diagram of our proposed HGA optimization method. Since the inverse scattering is an ill-posed problem, the solution is non-unique. Therefore, to reduce the search space and regularize the problem, we combined BGA and RGA. First, we start with a BGA procedure until a given stop condition is reached, and then the best candidate solutions found by BGA are chosen as an initial estimate in the first generation of RGA. One of the most critical points for accuracy in image reconstruction is the ability to accurately measure the field at the observation points. Moreover, measurement is always under the influence of external electromagnetic artifacts, which might change the measured scattered field. As well, due to the instability of the inverse problem, the image accuracy might decrease and non-real solution might be resulted by the reconstruction methods. However, the fine-tune capability of RGA in hybrid BGA/RGA improves the image accuracy in the presence of noise in the measurements. We recommend the HGA inverse solver for those applications that deal with complex and large distribution of dielectric properties.

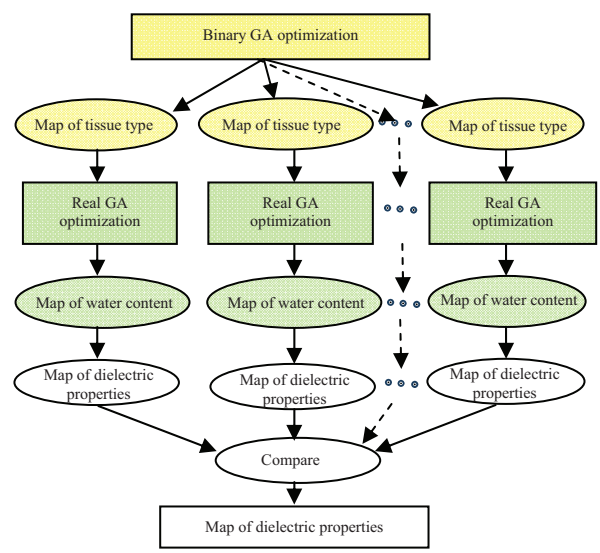

Fig. 3. Block diagram of HGA optimization method.

IV. INVERSION RESULTS

While the ultimate test of any inversion algorithm must involve experimentally collected scattered fields, for validation purpose it is very

useful to have a synthetic data set where the true image is known. We have created synthetic scattered data from a breast model that include a tumour. This application has been chosen due to the heterogeneous structure and dispersive characteristics of the breast. However, the proposed technique can be applied to many other applications. In the MWT imaging technique for breast cancer detection, the patient lies in prone position and the transmitter and receiver antennas are located on a circle around the uncompressed breast (Fig. 4). One antenna transmits a short, low-power microwave pulse and the receiver antennas collect the scattered field around the breast. The scattered signals are then processed to create a two-dimensional image. While a realistic model of the numerical breast phantom should be three-dimensional, two-dimensional models are quite prevalent mainly due to their simplicity [6, 7]. Also, a three-dimension image can be generated using a set of two-dimension images.

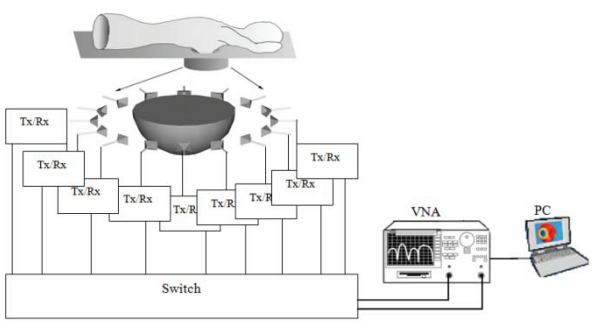

Fig. 4.Clinical imaging system configuration for MWT.

For simulations in this paper, the following parameters have been used. The mesh used for $(FD)^2TD$ simulations consists of 600 × 600 pixels chosen based on the size of the breast. The cell size (for inversion) is $\Delta = 0.5$ *mm*, which is $\lambda/10$ (where λ is the effective wavelength in the breast tissues at f=10GHz), and the time step is Δt=0.8*ps*. Increasing the resolution for the inversion will increase the size of the search space, and consequently, the computational cost. We utilized multiple-frequencies in our techniques for the frequency band between 3 GHz–10GHz, in 1 GHz steps. To enhance the accuracy of the image and reduce the ill-posedness of the problem, four different incident angles (0°, 90°, 180°, and 270°) have been used (the plane wave rotates 90° for each measurement). With respect to the number of the receivers, increasing the number of receivers provides more information about the object at almost no computational cost. In these simulations there are 100 observation points located in the far-field zone, and the time domain scattered field is measured on a circle around the numerical breast phantom with uniform spacing in the step of 3.6^o. From a practical point of view, using 100 probe positions at the observation points around the breast may not be possible in reality due to the size of antenna and mutual coupling between them. We chose this number for the proof of concept. Since we are interested in creating an image of the inner structure of objects,we limit our search space to only the interior of the object. In order to do this, information about the position, dimension, orientation, and surface of the object is required. This information can be found using surface detection methods [16, 17]. This information will be used in the inverse program in order to discretize only inside the object.

The dielectric properties of different tissue types, including normal, malignant, and benign breast tissues were obtained from reduction and cancer surgeries, in the frequency range of 0.5 GHz–20GHz, performed by Lazebnik*et al.* [13, 14]. Figure 5 shows the dielectric properties of different breast tissues created based on Debye model having different levels of water content for 3 GHz–10GHz. As can be seen in this figure, breast tissues may exhibit very low to very high loss at microwave frequencies. These variations depend on the tissue type, and more precisely, on the water content. The water dependency of dielectric properties of breast tissues can be efficiently described in $(FD)^2TD$ numerical method by using the single-pole Debye model [15],

$$\varepsilon = \varepsilon_0 (\varepsilon_\infty + \frac{\varepsilon_s - \varepsilon_\infty}{1 + j\omega\tau_0} - j\frac{\sigma_s}{\omega\varepsilon_0}) \qquad (2)$$

where ε_0 is the permittivity of the free space, ε_s and ε_∞ are the dielectric constants at zero (static) and infinite frequencies, respectively. σ_s is the conductivity at low frequency, ω is the angular frequency, and τ_0 is the relaxation time constant. In order to simplify the problem, the breast tissues are divided into seven groups: three different groups of fibro-glandular tissues, three different

groups of fatty tissues, and one transitional group (Fig. 5). Each group has an upper bound and a lower bound value of dielectric properties, depending on the amount of water content and the frequency. The dielectric properties can be given by,

$$\varepsilon(\omega) = p\varepsilon_u(\omega) + (1-p)\varepsilon_l(\omega) \tag{3}$$

$$(\omega) = p\sigma_u(\omega) + (1-p)\sigma_l(\omega), \tag{4}$$

where the parameter p is a coefficient showing the percentage of water content and it can vary between [0-1], ε_u and σ_u are the relative permittivity and conductivity at the upper bound, respectively, and ε_l and σ_l are the relative permittivity and conductivity at the lower bound of the corresponding group at a specific frequency, respectively.

Therefore, by substituting equations (3) and (4) into the first-order Debye formula the parameters of the Debye model become functions of both water content and the dielectric properties of the lower and upper bounds of each group, can be defined as,

$$\sigma_s = p\sigma_{us} + \sigma_{sl} - p\sigma_{sl} \tag{5}$$

$$\varepsilon_\infty = p\varepsilon_{\infty u} + \varepsilon_{\infty l} - p\varepsilon_{\infty l}, \tag{6}$$

$$\varepsilon_s = p\varepsilon_{us} + \varepsilon_{sl} - p\varepsilon_{sl}, \tag{7}$$

where σ_{su} and σ_{sl} are conductivity at the upper and lower bounds of the corresponding group, respectively, $\varepsilon_{\infty u}$ and $\varepsilon_{\infty l}$ are permittivity at infinite frequency for the upper and lower bounds of the corresponding group, and ε_{su} and ε_{sl} are relative permittivity at zero frequency for the upper and lower bounds of the corresponding group, respectively. The single-pole Debye parameters for the breast tissues are based on the results described by Zastrow*et al.* [18, 19]. At this point, by substituting the new parameters of the Debye model, the water content dependency has been included in $(FD)^2TD$ program.

In the following example, we examined the HGA for solving the inverse scattering problem for breast cancer imaging. The HGA is divided into two steps of optimization. At the first step, the BGA is employed in order to determine the type of the tissue for each cell of search space. In the second step, by using RGA, percentages of water content is found. In the BGA, the look-up table consists of first-order Debye parameters for four different tissue types: fibro-glandular, fatty, transitional, and malignant tissues with the water content percentage of 50 %, given in Table I. Note that in this table we combined all three groups of fibro-glandular tissues into one group of fibro-glandular tissue and all three groups of fatty tissues into one group of fatty tissue and we chose the Debye parameters of the corresponding tissue with 50 % water content.

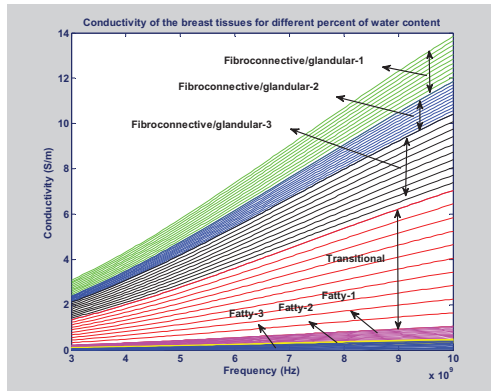

(a)

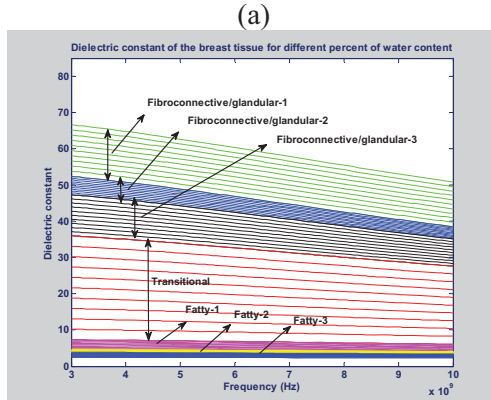

(b)

Fig. 5. Debye model of breast tissues dielectric properties (a) conductivity and (b) permittivity.

Table I. Look-up table of the Debye parameters for the BGA.

Medium	Fat	Transitional	Fibro-glandular	Malignant
ε_∞	4.33	22.46	52.02	76.17
ε_s	2.98	8.48	14.00	25.52
$\sigma_s(S/m)$	0.02	0.23	0.78	1.20
τ_0	13.0	13.0	13.0	13.0

The BGA optimization stops when the fitness value does not improve after some number of generations. Then, the best individuals of the last generation in terms of fitness value are passed to the second stage of the optimization, which is RGA. After the process of BGA, the behavior of

the best fitness values at different generations for each individual are studied to choose those individuals that show an increase in the fitness value consistently, and they were passed to RGA. This selection can decrease the chances of getting stuck in a local minimum and can increase the chance of finding the global optimum solution. For the RGA, the look-up table consists of first-order Debye parameters from the upper to lower end of the range for four different types of breast tissue (Table II).

Table II. Look-up table of the Debye parameters for the RGA.

Medium	Fat	Transitional	Fibro-glandular	Malignant
$\varepsilon_{\infty u}$	3.987	12.990	23.200	9.058
ε_{su}	7.535	37.190	69.250	60.360
$\sigma_{su}(S/m)$	0.080	0.397	1.306	0.899
$\varepsilon_{\infty l}$	2.309	3.987	12.990	23.200
ε_{sl}	2.401	7.535	37.190	69.250
$\sigma_{sl}(S/m)$	0.005	0.080	0.397	1.306
$\tau_0(ps)$	13.0	13.0	13.0	13.0

In this stage, for those individuals that are chosen by BGA, the tissue types remain constant, but the percentage of water content (p) can vary between 0% and 100%. RGA uses $p_i i=1,2,...n$ as genes. A combination of n gene gives a chromosome, where p is a floating point number between 0 and 1. Then equations (3), (4), and Table II are used to find tissue properties. Figure 6 shows a sub-sampled version of a cross-section of an MRI in the numerical breast phantoms repository of [20]. The measurement scattered field values are replaced by simulated data (hypothetical measured data) obtained by the Richmond method [21] to avoid the inverse crime. A 2D cross-section of a breast is divided into 18 equal regions.

In the first stage of the optimization process, typical Debye parameters are assigned to each category of the tissue type (fatty, transitional, fibro-glandular) assuming 50 % water content (Table I). Then, the BGA is used to find the tissue type. The best 4 solutions are then passed to the second stage where the RGA is used to find the water content. In this stage, the search space is limited to the range of the dielectric properties of each tissue type. After 200 generations of the RGA, the best candidate is chosen for further calibration and the other three candidates are removed from the optimization process. For the winning candidates, the GA runs for 300 more generations to obtain the final result. Parallel programming is used in RGA [22, 23].

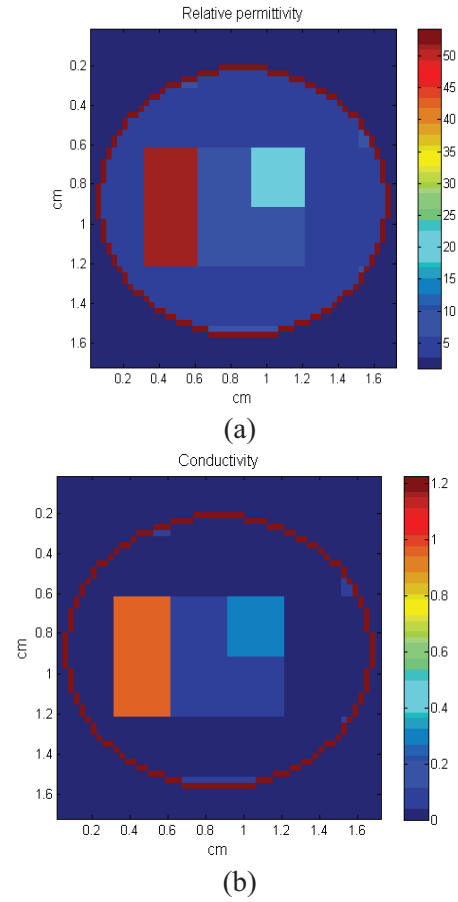

Fig. 6. (a) Relative permittivity and (b) conductivity of the numerical breast phantom obtained by sub-sampled breast MRI at $f = 6$ GHz.

Figure 7 (a) shows the average fitness value of the solutions of the BGA over 200 generations. Figure 7 (b) shows the improvement of the 4 candidates after 300 generations. The fitness value of one of the candidates significantly improves while for the other 3 do not show a significant improvement. This implies that for those candidates, the tissue type was not predicted correctly in the first stage. Figure 8 shows the reconstructed dielectric properties of the phantom shown in Fig. 6. It shows that the hybrid technique was able to correctly recognized the tissue types but the amount of water content was slightly different from the original image. This is due to the limited number of generations that we considered in this example.

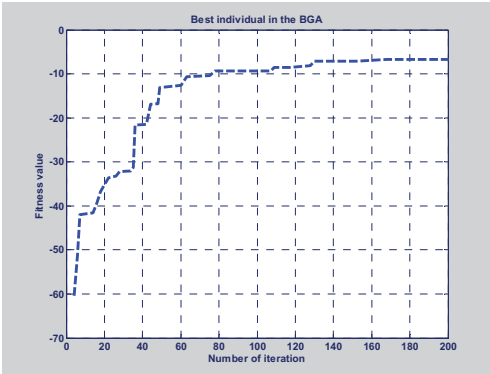

(a)

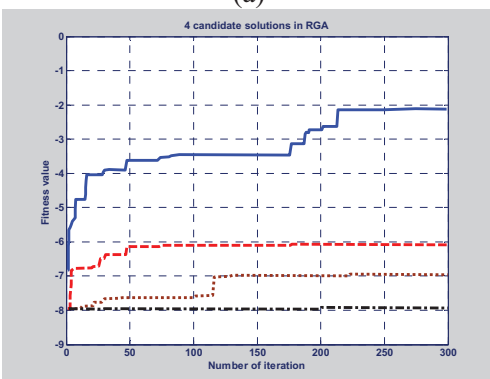

(b)

Fig. 7. (a) Trajectory of the fitness value of the best individual in the BGA and (b) trajectory of the fitness value of the 4 candidate solutions passed to RGA.

Two other optimization methods using BGA only and RGA only are implemented for comparison purposes. The hybrid method overall performs (4 (angle) × 30 (individual) × 200 (BGA generation) + (4(angle) × (individual) × 300 (RGA generation) = 60,000 function evaluations. In order to be comparable with the hybrid method, the BGA and the RGA should run for 500 generations with 30 individuals in each iteration. This results in 60,000 function evaluations. In this case, we used Table I for BGA and for the RGA, we considered the reconstructed relative complex permittivity within physical ranges $1.0 \leq \varepsilon_r \leq 80.0$ and $0.0 \leq \sigma \leq 15.0$ S/m, with one decimal point accuracy. Figure 9 shows the result of the BGA and the RGA after 500 generations. Neither of these methods (RGA alone or BGA alone) was able to converge to the right solution within 500 iterations. In addition, because four cases are optimized in parallel by RGA, the hybrid method is faster than both BGA and RGA alone. The convergence of the examples provided in this paper by using 64 nodes and 64G RAM took around four hours and thirty minutes.

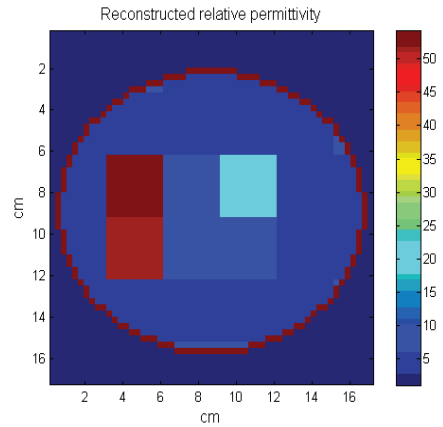

(a)

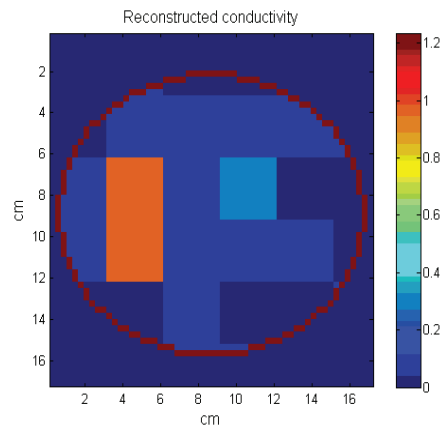

(b)

Fig. 8. Result of the HGA method for the numerical phantom of Fig. 6 (a) permittivity and (b) conductivity at $f = 6$ GHz.

In breast imaging, the typical range of the dielectric properties is limited and is determined by *a-priori* knowledge about the tissues existing in the breast. By limiting the search space to first finding the tissue type and then finding the water content for a specific tissue type, the proposed method decreases the possibility of the non-physical solutions from the search space. This is an advantage over many of the local optimization methods used in inverse scattering, and those that use a regularization terms with smoothing effects. Additionally, the proposed method is potentially able to reconstruct sharp profiles, which occur frequently in breast imaging.

From a practical point of view, the use of the 2D-TM approximation for what is really a 3D problem will introduce modeling error into the utilized inversion algorithm. Therefore, the modeling calibration is required to reduce the error. While reducing the model error is feasible, it needs substantial additional work that is beyond the scope of this paper. In this section, we propose ways to do the modeling calibration. Modeling calibration is the process of adjusting the raw 3D scattered field data such that it can be effectively employed by the approximate 2D models upon which the inversion algorithms are based. To reduce this modeling error, effort needs to be placed on calibrating the 3D model into 2D approximation. We need to introduce a calibration step (modeling calibration) in order to eliminate some of the experimental errors affecting field measurements, such as antennas, mutual coupling between co-resident non-active antennas, and the effects of boundaries on antenna characteristics. In order to calculate the calibration factor, we should have modeled the entire setup including the antennas and boundary using a more accurate (but much slower) 3D numerical technique for a given chamber configuration and the calibration factors should be provided as an input to the inversion algorithms without slowing them down. This procedure of simulating the 3D of the entire imaging chamber can be expedited using symmetric algorithm [24]. The modeling calibration is made for efficiency, because the behavior of electric fields within a 2D environment can be easily described with 2D FDTD and it can be repeatedly evaluated very quickly (when compared to a much slower 3D techniques) allowing the iterative imaging algorithms to converge to a solution in a reasonable amount of time.

V. CONCLUSION

In breast imaging, the typical range of the dielectric properties is limited and are determined by *a-priori* knowledge about the tissues existing in breast. By limiting the search space to first finding the tissue type and then finding the water content inside the range of the dielectric properties of that tissue type, the proposed method enables non-physical solutions to be removed from the search space. This is in contrast with many of the local optimization methods that are used in inverse scattering, which use a regularization term with smoothing effects. Hence, the proposed method is potentially able to reconstruct sharp profiles that occur frequently in breast imaging.

In conclusion, the proposed hybrid binary-real genetic algorithm increases the convergence speed in the application of microwave imaging for breast cancer. This method uses *a-priori* knowledge of the dielectric properties of the breast tissue and inherent advantage of binary GAs in discrete search spaces and real GAs in continuous search spaces.

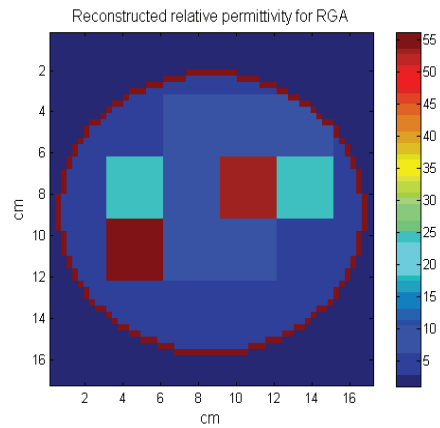

(a)

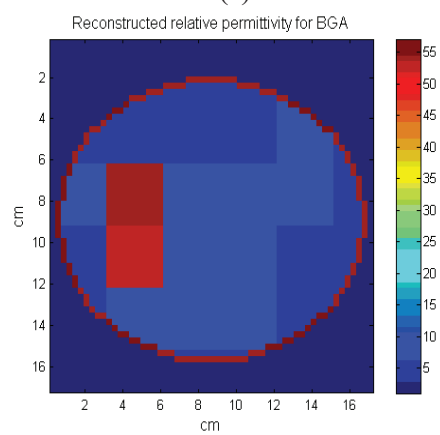

(b)

Fig. 9. Result of the (a) RGA and (b) BGA methods for relative permittivity at $f = 6$ GHz.

ACKNOWLEDGMENT

The authors would like to acknowledge the financial support of Wilkes University, Natural Sciences and Engineering Research Council of Canada, Cancer Care Manitoba, and University of North Dakota. Also constructive discussions with

Dr. L. Shafai and Dr. P. Thulasiraman are greatly appreciated.

REFERENCES

[1] M. Pastorino, "Stochastic optimization methods applied to microwaveimaging: A review," *IEEE Trans. Antennas Propagat.*, vol. 55, no. 3, pp. 538-548, 2007.

[2] A. Sabouni, S. Noghanian, and S. Pistorius, "A global optimization technique for microwave imaging of the inhomogeneous and dispersivebreast," *Canadian Journal of Electrical and Computer Engineering*, vol. 35, no.1, pp. 15-24, 2010.

[3] A. Sabouni, A. Ashtari, S. Noghanian, G. Thomas, and S. Pistorius, "Hybrid binary-real GA for microwave breast tomography," *IEEE Antennas and Propagation Society International Symposium*, 2008.

[4] A. Ashtari, S. Noghanian, A. Sabouni, and G. Thomas, "Hybrid binary real genetic algorithms for microwave image reconstruction," *24th Annual Review of Progress in Applied Computational Electromagnetics Society*, pp. 116-121, Niagara Falls, Canada, 2008.

[5] A. Sabouni and S. Noghanian, "Study of penetration depth and noise inmicrowave tomography technique," *Applied Computational ElectromagneticsSociety (ACES) Journal*, vol. 28, no. 5, pp. 391-403, 2013.

[6] T. Rubk, P. Meaney, P. Meincke, and K. Paulsen, "Nonlinear microwave imaging for breast-cancer screening using Gauss-Newton's method and the CGLS inversion algorithm," *IEEE Trans. Antennas Propagat.*, vol. 55, no. 8, pp. 2320-2331, 2007.

[7] P. Meaney, K. Paulsen, S. Geimer, S. Haider, and M. Fanning, "Quantificationof 3-d field effects during 2-d microwave imaging," *IEEE Trans. Biomed. Eng.*, vol. 49, no. 7, pp. 708-720, 2002.

[8] A. Sabouni, S. Noghanian, and L. Shafai, "Transverse electric and magnetic components of field measurement for microwave breast cancerimaging," *International Symposium on Antenna Technology and Applied Electromagnetics the American Electromagnetics Conference*, Ottawa, Canada, 2010.

[9] A. Taflove and S. C. Hagness, *Computational Electrodynamics: The Finite-Difference Time-Domain* Method, 3rd ed. Artech House, Norwood, 2005.

[10] A. Elsherbeni and V. Demir, *The Finite Difference Time Domain Method for Electromagnetics: With MATLAB Simulations*, SciTech Publishing Inc., 2009.

[11] M. Bui, S. Stuchly, and G. Costache, "Propagation of transients indispersive dielectric media," *IEEE Trans. Microw. Theory Tech.*, vol. 39, no. 7, pp. 1165-1172, 1991.

[12] A. Sabouni, S. Noghanian, and S. Pistorius, "Frequency dispersion effects on FDTD model for breast tumor imaging application," *IEEE International Symposium on Antennas and Propagation*, pp. 1410-1413, 2006.

[13] M. Lazebnik, L. McCartney, D. Popovic, B. Watkins, M. Lindstrom, J. Harter, S. Sewall, A. Magliocco, J. Booske, M. Okoniewski, and S. Hagness, "Large-scale study of the ultra wideband microwave dielectric properties of normal breast tissue obtained from reduction surgeries," *Physics in Medicine and Biology*, vol. 52, pp. 2637-2656, 2007.

[14] M. Lazebnik, D. Popovic, L. McCartney, C. Watkins, M. Lindstrom, J. Harter, S. Sewall, T. Ogilvie, A. Magliocco, T. Breslin, D. Temple, W. Mew, J. Booske, M. Okoniewski, and S. Hagness, "Alarge-scale study of the ultra wideband microwave dielectric properties of normal, benign, and malignant breast tissues obtained from cancer surgeries," *Physics in Medicine and Biology*, vol. 52, pp. 6093-6115, 2007.

[15] A. Sabouni, S. Noghanian, and S. Pistorius, "Water content and tissue composition effects on microwave tomography results," *International Review of Progress in Applied Computational Electromagnetics (ACES)*, 2008.

[16] D. Woten and M. El-Shenawee, "Quantitative analysis of breast skinfor tumor detection using electromagnetic waves," *Applied Computational Electromagnetics Society (ACES) Journal*, vol. 24, no. 5, pp. 458-463, 2009.

[17] T. Williams, J. Sill, J. Bourqui, and E. Fear, "Tissue sensing adaptive radar for breast cancer detection: Practical improvements," *IEEE International Symposium on Antennas and Propagation*, 2010.

[18] E. Zastrow, S. Davis, M. Lazebnik, F. Kelcz, B. Veen, and S. Hagness, "Database of 3d grid-based numerical breast phantoms for use in computational electromagnetics simulations," *Instruction manual*, 2007.

[19] E. Zastrow, S. Davis, M. Lazebnik, F. Kelcz, B. Veen, and S. Hagness, "Development of anatomically realistic numerical breast phantoms with accurate dielectric properties for modeling microwave interactions with the human breast," *IEEE Trans. Biomed. Eng.*, vol. 55, no. 12, pp. 2792-2800, 2008.

[20] E. Zastrow, S. Davis, M. Lazebnik, F. Kelcz, B. Veen, and S. Hagness, "Database of 3D grid-based numerical breast phantoms foruse in

computational electromagnetics simulations," *Instruction Manual*, University of Wisconsin-Madison.

[21] J. Richmond, "Scattering by a dielectric cylinder of arbitrary cross sectionshape," *IEEE Trans. Antennas Propagat*., vol. 13, no. 3, pp. 334-341, 1965.

[22] M. Xu, A. Sabouni, P. Thulasiraman, S. Noghanian, and S. Pistorius, "Image reconstruction using microwave tomography for breast cancer detection on distributed memory machine," *International Conferenceon Parallel Processing*, 2007.

[23] ——, "A parallel algorithmic approach for microwave tomography inbreast cancer detection," *IEEE International Parallel and Distributed Processing Symposium*, pp. 1-8, 2007.

[24] A. Sabouni, M. Pavlovic, M. Ostadrahimi, and S. Noghanian, "Three dimensional accurate modeling of the microwave tomography imaging system," *IEEE Antenna Propagation International Symposium*, Spoken, USA, 2007.

Abas Sabouni received the M.Sc. degree inelectrical engineering from K. N. Toosi University, Tehran, Iran, in 2005, and Ph.D. degreein electrical engineering, from the Universityof Manitoba, Winnipeg, MB, Canada, in 2011. Since 2013, he has been an Assistant Professor in the Departmentof Electrical Engineering and Physics, Wilkes University, Wilkes-Barre, PA, USA. From 2010 to 2013, he was a Post-Doctoral Fellow in Biomedical Engineering Department at the Ecole Polytechnique de Montreal, and Research Associate at the Department of Electricaland Computer Engineering at the Concordia University. He was a Research and Development Engineer at Parto Dadeh Inc., Tehran, Iran during 2001 through 2004. During 2005 and 2006, he was a Research Assistant in the Electromagnetic Group, Universityof Manitoba and a Research Associate at Cancer Care Manitoba. From 2009 to 2010, he was a Research Associate in the Department of Electrical Engineering, University of North Dakota, Grand Forks, North Dakota, USA. His research interests include inverse scattering problem, microwave imaging, UWB antenna design and modeling, and transcranial magnetic stimulation. Dr. Sabouni is the recipient of the IEEE AP-S Honorable Mention Student Paper Contest 2008. In 2013, he served as the Vice-President of IEEE Montreal section. From 2010 to 2013, he was the Chair of IEEE Montreal Antenna Propagation Chapter.

Ali Ashtari received bachelor and masters of science in Electrical Engineering from Sharif University of Technology, Iran and a PhD in Electrical and Computer Engineering from University of Manitoba, Canada in 2001, 2004 and 2009 respectively. He is currently the Research Lead at Invenia Technical Computing. Ali has extensive academic (Ph.D) and industrial experience in signal processing, statistics, numerical methods and optimization applied to various problems ranging from biomedical applications and renewable energy to electricity markets.

Sima Noghanian received the B.Sc. degree in Electrical Engineering from the Sharif Universityof Technology, Tehran, Iran, in 1992, and the M.Sc. and Ph.D. degrees, both in Electrical Engineering, from the University of Manitoba, Winnipeg, Canada, in 1996 and 2001, respectively. In 2001, she was at Yotta Yotta Corporation, Edmonton, Canada. She was an Assistant Professor in the Department of Electrical Engineering, Sharif University of Technology during 2002 and 2003. From 2003 to 2008, she was an Assistant Professor in the Departmentof Electrical and Computer Engineering, University of Manitoba. Since 2008, she has been an Assistant Professor in the Departmentof Electrical Engineering, University of North Dakota, Grand Forks. Her research interests include antenna design and modeling, wireless channel modeling, ultrawideband antennas, and microwave imaging. Dr. Noghanian was IEEE Winnipeg Waves (joint Chapter of Antennaand Propagation/Microwave Theory and Techniques/Vehicular Technologysocieties) Chapter Chair during 2004 and 2005. She received a Postdoctoral Fellowship from Natural Sciences and Engineering Research Council of Canada at the University of Waterloo in 2002.

Gabriel Thomas received the B.Sc. degree in Electrical Engineering from the Monterrey Institute of Technology, Monterrey, Mexico, in 1991, and the M.Sc. and Ph.D. degrees in Computer Engineering from the University of Texas, El Paso, in 1994 and 1999, respectively. Since 1999, he has been a faculty member in the Department of Electrical and Computer Engineering, University of Manitoba,

Winnipeg, MB, Canada, where he is currently an Associate Professor. He is coauthor of the book "Range Doppler Radar Imaging and Motion Compensation". His current research interests include digital image and signal processing, computer vision and nondestructive testing.

Stephen Pistorius is a Physics Professor and an Associate Professor of Radiology at the University of Manitoba (UM) and a Senior Scientist at Cancer Care Manitoba (CCMB). Educated in South Africa, he holds B.Sc., Hons. B.Sc. (Radiation Physics), M.Sc. (Medical Physics) and Ph.D. degrees. Prior to certifying as a Medical Physicist in 1986 he worked in industry. He practiced in Cape Town before moving to Canada as a Senior Medical Physicist at CCMB. In 1995 he was appointed Director of Medical Physics and was promoted to Provincial Director in 2000, an executive position which oversaw 70+ staff responsible for RT Physics, Imaging, Radiation Protection, Engineering, Teaching and Research. He is a Senior Member of the IEEE and a professional physicist and in 2005 he obtained a Post-Graduate Diploma in Business Administration from the Edinburgh Business School. Prof. Pistorius served as the President of the Canadian Organization of Medical Physicists (COMP) and is currently the Director of Professional Affairs for the Canadian Association of Physicists. In 2010 he chose to focus on research and teaching and currently serves as the Director of the UM Medical Physics graduate program and Vice-Director of the Biomedical Engineering graduate program. Prof. Pistorius uses fundamental physics to improve and quantify diagnostic and therapeutic techniques and is interested in radiation transport in clinical imaging and treatment modalities. He has supervised and examined 30+ graduate students and currently advises 3 PDF's and 10 graduate students working on cancer imaging research; developing systems for cancer diagnosis which use photon scattering to enhanced CT and PET; microwave imaging and the use of MV radiation to image RT patients to optimize treatments by accounting for motion. He is the author of over 170 publications and presentations, serves on many scientific advisory boards and grant review panels and has a number of national and international awards to his name. In 2012 he was honored as a Fellow of COMP.